Brassica juncea plant cadmium resistance 1 protein (BjPCR1) facilitates the radial transport of calcium in the root

Song, W-Y ; Choi, K-S ; Alexis, D A ; Martinoia, E ; Lee, Y

Abstract: Calcium (Ca) is an important structural component of plant cell walls and an intracellular messenger in plants and animals. Therefore, plants tightly control the balance of Ca by regulating Ca uptake and its transfer from cell to cell and organ to organ. Here, we propose that Brassica juncea PCR1 (PCR1), a member of the plant cadmium resistance (PCR) protein family in Indian mustard, is a Ca(2+) efflux transporter that is required for the efficient radial transfer of Ca(2+) in the root and is implicated in the translocation of Ca to the shoot. Knock-down lines of BjPCR1 were greatly stunted and translocated less Ca to the shoot than did the corresponding WT. The localization of BjPCR1 to the plasma membrane and the preferential expression of BjPCR1 in the root epidermal cells of WT plants suggest that BjPCR1 antisense plants could not efficiently transfer Ca(2+) from the root epidermis to the cells located inside the root. Protoplasts isolated from BjPCR1 antisense lines had lower Ca(2+) efflux activity than did those of the WT, and membrane vesicles isolated from BjPCR1-expressing yeast exhibited increased Ca(2+) transport activity. Inhibitor studies, together with theoretical considerations, indicate that BjPCR1 exports one Ca(2+) in exchange for three protons. Root hair-specific expression of BjPCR1 in Arabidopsis results in plants that exhibit increased Ca(2+) resistance and translocation. In conclusion, our data support the hypothesis that BjPCR1 is an exporter required for the translocation of Ca(2+) from the root epidermis to the inner cells, and ultimately to the shoot.

DOI: https://doi.org/10.1073/pnas.1104905108

Originally published at:
Song, W-Y; Choi, K-S; Alexis, D A; Martinoia, E; Lee, Y (2011). Brassica juncea plant cadmium resistance 1 protein (BjPCR1) facilitates the radial transport of calcium in the root. Proceedings of the National Academy of Sciences of the United States of America (PNAS), 108(49):19808-19813.
DOI: https://doi.org/10.1073/pnas.1104905108

Biological Science / Plant Biology

Brassica juncea PCR1 facilitates the radial transport of calcium in the root

Won-Yong Song[1,2,3], Kwan Sam Choi[3], De Angeli Alexis[1], Enrico Martinoia[1,2,&] and Youngsook Lee[2&]

[1]Institute of Plant Biology, University Zurich, Zollikerstrasse 107, 8008 Zurich, Switzerland
[2]POSTECH-UZH Cooperative Laboratory, Department of Integrative Bioscience and Biotechnology, World Class University Program, Pohang University of Science and Technology, Pohang, 790-784, Korea
[3]Division of Applied Biology, College of Agriculture and Life Sciences, Chungnam National University, Daejeon 305-764, Korea

[&]equally contributing corresponding authors:
Youngsook Lee: ylee@postech.ac.kr;
Enrico Martinoia: Enrico.Martinoia@botinst.uzh.ch

Running Title: BjPCR1 contributes to radial calcium transfer in roots

Estimated length of the manuscript: 6 pages

Keywords:
Indian mustard , BjPCR, Ca^{2+}-efflux transporter, Ca translocation, plasma membrane H^+/Ca^{2+} antiporter

Ca is an important structural component of plant cell walls and an intracellular messenger in plants and animals. Therefore, plants tightly control the balance of Ca, by regulating Ca uptake and its transfer from cell to cell and organ to organ. Here, we propose that *Brassica juncea PCR1* (*BjPCR1*), a member of the Plant Cadmium Resistance (PCR) protein family in Indian mustard, is a Ca^{2+} efflux transporter that is required for the efficient radial transfer of Ca^{2+} in the root, and is implicated in the translocation of Ca to the shoot. Knock-down lines of *BjPCR1* were greatly stunted, and translocated less Ca to the shoot than did the corresponding wild type. The localization of BjPCR1 to the plasma membrane and the preferential expression of *BjPCR1* in the root epidermal cells of wild-type plants suggest that *BjPCR1* antisense plants could not efficiently transfer Ca^{2+} from the root epidermis to the cells located inside the root. Protoplasts isolated from *BjPCR1* antisense lines had lower Ca^{2+} efflux activity than did those of the wild type, and membrane vesicles isolated from

***BjPCR1*-expressing yeast exhibited increased Ca^{2+} transport activity. Inhibitor studies, together with theoretical considerations, indicate that BjPCR1 exports one Ca^{2+} in exchange for three protons. Root hair-specific expression of *BjPCR1* in Arabidopsis results in plants that exhibit increased Ca^{2+} resistance and translocation. In conclusion, our data support the hypothesis that BjPCR1 is an exporter required for the translocation of Ca^{2+} from the root epidermis to the inner cells, and ultimately to the shoot.**

\body Calcium (Ca) is an essential nutrient for plants. It is required for Ca^{2+}-mediated signal transduction, the stabilization of the cell wall and plasma membrane, ion balance, and vacuolar osmoregulation (1-3). The diverse functions of Ca^{2+} in the plant require that the concentration of Ca^{2+} be maintained and regulated differently in different compartments, and in a timely manner, and this is achieved by the activity of numerous Ca transporters.

Ca^{2+}-mediated signal transduction is necessary for the proper response of plants to touch, cold, and drought, and for the closure of stomata in response to ABA, cold, and atmospheric CO_2 (4-5). Ca^{2+}-mediated signal transduction is often initiated by rapid Ca^{2+} influx through selective or non-selective Ca^{2+} channels located in the plasma membrane and intracellular organelles, such as the Ca^{2+}-permeable outward-rectifying K^+ channel (KORC), depolarization-activated Ca^{2+} channel (DACC), hyperpolarization-activated Ca^{2+} channel (HACC), and voltage-dependent Ca^{2+} channel (VIC) (4, 5). In order that changes in Ca^{2+} concentration are perceived as a signal, the cytosolic Ca^{2+} concentration has to be maintained at submicromolar concentrations. Such a low cytosolic Ca^{2+} concentration can be maintained by Ca^{2+} efflux transporters, such as Ca^{2+}-ATPases (ECA1, ACA1, and ACA4) and H^+/Ca^{2+} antiporters (CAXs) at the ER membrane and tonoplast, respectively (2, 5), and Ca^{2+}-ATPases and H^+/Ca^{2+} exchangers at the plasma membrane (6, 7).

In contrast to this need of individual cells to maintain cytosolic Ca^{2+} at very low level, large quantities of Ca^{2+} are needed at the whole plant level, due to the structural role that Ca^{2+} plays in stabilizing cell walls and the plasma membrane, and also due to its function as a counter-ion for the massive amount of anions in the vacuole. In crops, the drop of Ca^{2+} levels to below a critical level in fast-growing tissues causes diseases such as black heart in *Apium graveolens* (celery), blossom end rot in *Solanum lycopersicum* (tomatoes), and bitter-pit in *Malus domestica*

(apples) (1, 2). These phenomena demonstrate the importance of regulating Ca^{2+} uptake and allocation. In the root, Ca^{2+} is taken up by epidermal cells, radially transferred to the inner parts of the root, and then finally loaded into the xylem for transport to the shoot. However, a detailed understanding of the mechanism underlying each step of Ca^{2+} transport is lacking. For example, it has been debated which part of the root is involved in Ca^{2+} uptake from the rhizosphere, and whether the apoplastic or symplastic pathway is the predominant route for Ca^{2+} transport across the endodermal layer of the root (8-10). It is also not known which transporters are necessary for xylem loading of Ca^{2+}.

In an effort to gain insight into the function of the Plant Cadmium Resistance (PCR) family, we identified two members of this family from *Brassica juncea*. We demonstrate that, although BjPCR1 exhibits strong sequence similarity to AtPCR2, which plays a role in heavy metal transport (11, 12), BjPCR1 is not involved in heavy metal transport, but contributes to Ca translocation from the root to the shoot via a Ca^{2+} efflux mechanism located in root epidermis.

Results

Identification of *Brassica juncea* PCRs

Previously, we identified and characterized two Plant Cadmium Resistance proteins (PCRs) involved in heavy metal homeostasis in Arabidopsis (11, 12). *Brassica juncea* is a crop with a high intrinsic heavy metal tolerance and accumulation (13, 14), and may therefore contain members of the PCR family with distinct characteristics. Because *Brassica* has coding sequences that are very similar to those of *Arabidopsis thaliana* (15), we used primers specific for *AtPCR1* to isolate *PCR* genes from *B. juncea* (11). Using a genomic PCR approach, we identified three different *BjPCR*s. All three *BjPCR* genes have four exons and three introns at the same positions as *AtPCR1* and *2* (Fig. S1). The lengths of the exons of the three *BjPCR* genes were very similar to those of *AtPCR1* and *2*. In contrast, the introns exhibited some variation. *Brassica* PCR1 was more similar to AtPCR2 than to AtPCR1 and exhibited 76% identity at the amino acid level with AtPCR2 (Fig. 1*A*). Due to the high overall identity between AtPCR1, AtPCR2, and BjPCRs, particularly in the hydrophobic domain, which contains the CCXXXXCPC (CC-CPC) motif shown to be required for

cadmium resistance (11), we expected that BjPCRs would also be implicated in conferring Cd resistance. To test this hypothesis, we isolated the corresponding *BjPCR1* and *2* cDNAs and expressed them in the cadmium-sensitive yeast mutant, DTY167. On normal 1/2 SG-agar medium, *BjPCR1*-, *BjPCR2*-, and *AtPCR2*-expressing yeast cells showed similar growth. Surprisingly, and in contrast to Arabidopsis *PCR2*, *BjPCR1* conferred only weak cadmium tolerance, and *BjPCR2* did not restore any tolerance at all to cadmium (Fig. S2*A*). To determine why BjPCR1 does not confer cadmium tolerance, we undertook domain swapping experiments with BjPCR1 and AtPCR2. The results showed that mBP1, a hybrid construct consisting of the N-terminal part of AtAPCR2 and the C-terminal part of BjPCR1, conferred cadmium tolerance (Fig. S2*B*). Site-directed mutagenesis analysis within the N-terminal part of BjPCR1 revealed that the exchange of the naturally occurring Q11 with a His residue resulted in a BjPCR1 form that conferred cadmium tolerance (Fig. S2*C*) and decreased cadmium content (Fig. S2*D*) in *ycf1* yeasts. Interestingly, the single amino acid change introduced to 11H-BjPCR1 caused a shift in the protein band mobility, while it did not change the protein level (Fig. *S2E*). This band mobility shift suggests a change in protein structure which might have contributed to the dramatic change in PCR function to confer Cd tolerance.

Phenotypic analysis of *BjPCR1* antisense lines

To investigate the physiological function of BjPCRs in *Brassica juncea*, we produced a silencing construct for *BjPCR1* and *2* that down-regulated the expression of both genes. We examined *BjPCR1* and *2* transcript levels in the roots of 20 transformants exhibiting bar gene-mediated phosphinothricin resistance, using RNA blot analysis with a *BjPCR1* probe which can cross react with both *BjPCR* genes. Based on the expression levels of *BjPCRs* (Fig. 1*B*), we selected two lines with the lowest transcript levels (lines 5 and 17) and one where the transcript levels were only partially decreased and which could be used as a control (line 8). When these plants were grown under hydroponic conditions, lines 5 and 17 exhibited impaired growth, whereas line 8 grew at similar rates as the wild-type plants (Fig. 1*C*). Quantification of the shoot and root biomass confirmed our visual impression (Fig. 1*D*). In lines 5 and 17, the shoot biomass was decreased by nearly 40%. The reduction in biomass

was even more pronounced at the root level, where the biomass of lines 5 and 17 decreased by more than 70% of wild-type values (Fig. 1*D*).

To determine the reason for this drastic phenotype, we first measured the levels of major cations in the mutant lines and wild-type plants grown under control conditions (Figs. 2 and S3). We did not detect any difference in cation content between our control anti-BjPCR1-8 plant and the wild type, which corresponded well with the absence of a difference in growth phenotype in this line. In contrast, we observed a pronounced difference in Ca, Fe, Mn and Na concentrations between anti-BjPCR1-5 and -17 and the corresponding wild type (Figs. 2*A* and S3*A*-*D*). Only a slight effect was detected for Mg^{2+}, while no differences were observed for Zn, Cu, and K (Figs. 2*B* and S3*E*-*F*). The most drastic differences between the silenced lines and wild-type plants were observed for Ca (Fig. 2*A*). Ca concentrations in anti-BjPCR1-5 and -17 were only 65-75% of those observed in the wild-type, whereas they were at least two fold higher than in the wild type in the root. Consequently, the shoot to root ratio of Ca^{2+} was dramatically altered in the anti-BjPCR1-5 and -17 lines, whereas that of other ions was less affected (Figs. 2*C* and S3*G*). A comparison of biomass (Fig. 1*D*) with Ca concentrations (Fig. 2*A*) revealed that the growth of roots of the antisense lines was strongly impaired despite the fact that they contained high levels of Ca^{2+}. This may be because either the high level of Ca^{2+} exerted a toxic effect, or that the shoot, which did not have sufficient levels of Ca^{2+}, could not develop normally, and thus failed to provide sufficient energy for root growth. The remarkable difference in the shoot to root ratio of Ca between the wild type and the antisense lines 5 and 17 indicated that BjPCR1 plays a major role in the transfer of Ca^{2+} from the root to the shoot, and thus differs from its Arabidopsis homologues, AtPCR2, which transport Zn (12). Therefore, we concentrated our further studies on the role of BjPCR1 in Ca^{2+} distribution and transport.

Ca^{2+} translocation in anti-BjPCR1 lines

To confirm the decreased root to shoot Ca translocation observed in the BjPCR1-5 and -17 lines, we performed short-term uptake experiments using $^{45}Ca^{2+}$ (Fig. 2*D* and *E*). When grown in hydroponic medium and exposed for 15 h to 0.4 MBq $^{45}Ca^{2+}$, the leaves of the anti-BjPCR1 mutant lines 5 and 17 contained less ^{45}Ca radioactivity than did those of the corresponding wild type (Fig. 2*D* and *E*). To test if BjPCR1 is involved in the lateral transport of Ca^{2+}, we analyzed Ca^{2+} distribution in

the root hair zone and root tip, where the Casparian band has not yet formed, using a cell-permeable Ca^{2+} dye, the acetoxymethyl ester derivative of fluo-3 (Fluo-3-AM). This dye permeates into cells, is hydrolyzed by non-specific esterases, and the cleavage product, fluo-3, emits a green fluorescence when bound to Ca^{2+}, allowing the visualization of intracellular Ca^{2+} (13).Roots of wild-type plants exhibited a strong Ca^{2+}-dependent fluorescence signal in the tip and epidermal layer of the tip (Fig. 2*F*). A Ca^{2+} signal was also observed in the stele. In the root hair zone of the root, the strongest Ca^{2+} signal was observed in the tissue inside the epidermis adjacent to the root tip and in the stele (Fig. 2*F*). In contrast, the Ca^{2+}-dependent fluorescence signal of the two anti-BjPCR1 mutant lines was less pronounced in the root tip. In the root hair zone, Ca^{2+}-dependent fluorescence could only be observed in the epidermal cells and root hairs, but not in the stele (Figs. 2*F* and S4). No difference in the fluorescence pattern of zinpyr-1, an indicator dye for zinc, was observed between the roots of the wild type and the antisense lines (Fig. S5), which corresponded with the absence of differences in Zn concentration in wild-type and mutant plants (Fig. 2*B*). Furthermore, this result indicates that the difference in the fluo-3 pattern between the antisense and wild-type lines did not originate from any difference in dye penetration. Taken together, these results suggest that anti-BjPCR1 lines do not efficiently translocate Ca^{2+} from the root epidermal cells to the inner cells of the root.

Tissue-specific expression of *BjPCRs*

To further understand the function of *BjPCR1* and *2* in *Brassica*, we analyzed the tissue-specific expression. *BjPCR1* was expressed mainly in roots, but was also present in leaves (Fig. 3*A*). Expression in stems and flowers was low. The expression pattern of *BjPCR2* was similar to that of *BjPCR1*, but the overall expression level was lower than that of *BjPCR1* (Fig. 3*A*). To obtain a clue as to where in the root *BjPCR1* and *2* are expressed, we first used a stepwise grinding method. *BjPCR1* was highly expressed in root hair cells, which fell off at the first step of grinding, and its expression pattern was similar to that of *EXP7,* a root hair marker (14), but was opposite to that of *HMA4,* which is mainly expressed in vascular tissues (15) (Fig. 3*B*). Whole-mount *in situ* RNA hybridization confirmed that *BjPCR1* is indeed strongly expressed in the epidermal layer (antisense probe of Fig. 3*C*). We cannot completely exclude the possibility that *BjPCR1* is also expressed in other parts of the root; however, in this case the expression level would be very low

compared to that in epidermal cells. The grinding method indicates that *BjPCR2* exhibits a similar expression pattern as *BjPCR1* (Fig. 3*B*), but the expression level of *BjPCR2* was one-tenth that of *BjPCR1* (Fig. 3*A*, *B* and *D*). *BjPCR1* was strongly induced under Ca^{2+} starvation conditions, but not under Ca^{2+} excess conditions (Fig. 3*D*). *BjPCR2* exhibited a similar response, but its expression level remained lower than that of *BjPCR1*.

Plasma membrane localization of BjPCR1-GFP

To investigate the subcellular localization of BjPCR1 *in planta*, transgenic Arabidopsis lines expressing the *35S::BjPCR1-GFP* construct were generated. Green fluorescence in the root epidermal cells of these plants was localized to the plasma membrane (Fig. 3*E*). Transient expression of the construct in tobacco epidermal cells by infiltration confirmed that BjPCR1-GFP was targeted to the cell surface in close proximity to the cell wall, which was stained with propidium iodide (PPI; Fig. 3*F*). These results indicate that BjPCR1-GFP is located at the plasma membrane of plant cells.

Ca^{2+}-transfer by BjPCR1 in the root epidermis

Ca^{2+} transport analysis and epidermal plasma membrane localization of *BjPCR1* indicated that BjPCR1 acts as a Ca^{2+} efflux transporter at the epidermis for shoot Ca^{2+} translocation in *B. juncea*. If BjPCR1 indeed facilitates Ca^{2+} efflux from the epidermis to the apoplast, the pathway for Ca^{2+} translocation to the shoot involves both the symplast of the epidermal cells and the adjacent apoplast. To estimate the portions of the apoplast/symplast combinatorial pathway and the entirely apoplastic pathway in the total transfer of Ca^{2+} to the shoot, we compared the short-term root uptake of ^{45}Ca at 0°C and 25°C. The results demonstrated that, although Ca^{2+} transport was significant at 0°C (70% for WT), which is probably through the apoplast alone, 30% of the transport is mediated by energy-dependent mechanism(s) that might include uptake into the epidermis and subsequent release into the cortical apoplast (Fig. S6, WT). Furthermore, the same temperature-dependent transport assays with antisense BjPCR1 lines 5 and 17 revealed that they contained higher levels of Ca^{2+} than the wild type, especially at 25°C (Fig. S6), which suggests that BjPCR1 is important for the energy-dependent removal of Ca^{2+} from the epidermis to the apoplast.

To test further whether Ca^{2+} is indeed a physiological substrate of BjPCR1 important for Ca^{2+} transfer at the epidermis, we expressed *BjPCR1* in Arabidopsis root hair cells using the *AtEXP7* promoter, and thereby generated *EXP2p::BjPCR1-V5* and *EXP2p::BjPCR1-GFP* transgenic plants. As shown in Figure 4*A*, BjPCR1-GFP was indeed specifically expressed in the root hair cells of these Arabidopsis plants. When *EXP2p::BjPCR1-V5* or *EXP2p::BjPCR1-GFP* transgenic Arabidopsis plants were grown on media containing different concentrations of calcium, manganese or iron, Arabidopsis plants expressing *BjPCR1* grew better than the wild type under the Ca^{2+}-deficient, -sufficient,-excessive and Mn^{2+}-excessive conditions, but grew similarly to wild type in medium containing excess iron (Figs. 4*B*, S7*A*, *B* and *E*). The most dramatic effect was observed when Ca^{2+} was present at high concentrations, which impaired plant growth (Figs. 4*B*, S7*A* and *B*). Ca^{2+} was present at higher concentrations in the shoots, but at similar concentrations in the roots of transgenic Arabidopsis lines relative to the wild type (Fig. S7*C*), resulting in an increase in shoot to root Ca ratio in the transgenic plants (Fig. 4*C*), and indicating that Ca^{2+} is translocated more efficiently in the transgenic plants. Together, these results indicate that Ca^{2+} is a physiological substrate of BjPCR1, and further suggest that, in the epidermis, BjPCR1 contributes to Ca^{2+} translocation to the shoot.

Ca^{2+} efflux activity by BjPCR1

To test whether BjPCR1 acts directly as a Ca^{2+} efflux transporter, we performed transport experiments using mesophyll protoplasts isolated from the anti-BjPCR1 lines and wild-type plants. The $^{45}Ca^{2+}$ uptake activity of protoplasts of the antisense lines was about twice that of control protoplasts (Fig. 5*A*). This result could indicate that the Ca^{2+} taken up by control plants is readily exported, whereas that taken up by antisense lines is not. To test this hypothesis, we preloaded protoplasts isolated from control and mutant plants for 30 min with $^{45}Ca^{2+}$ and then investigated the release of $^{45}Ca^{2+}$. Indeed, Ca^{2+} efflux rates were slower in protoplasts isolated from antisense lines than in those from wild-type plants (Fig. 5*B*), indicating that BjPCR1 acts as a Ca^{2+} efflux transporter, and supporting the conclusions drawn from the experiments on whole plants.

To further confirm that BjPCR1 is indeed a Ca^{2+} transporter, we expressed *BjPCR1* in the yeast strain SM17, which is deficient in CNB1 and the Ca^{2+} transporters, PMR1, PMC1, and VCX1. The ^{45}Ca uptake experiment in the *BjPCR1*-

expressing yeast cells showed that BjPCR1 decreased the Ca^{2+} content of the cell (Fig. S8*A*), which indicated that BjPCR1 had a role in Ca^{2+} efflux. This result is also consistent with the increased Ca^{2+} level in protoplasts isolated from anti-BjPCR1 lines (Fig. 5*A*). For the in-depth analysis of BjPCR1-mediated transport, vesicles were isolated from yeast cells and used in the Ca^{2+} transport assay. The vesicles prepared from yeast cells expressing BjPCR1 exhibited significantly increased Ca^{2+} transport activity relative to those isolated from the empty vector control. During the first 30 min of incubation, yeast vesicles expressing *BjPCR1* took up Ca^{2+} about four times faster than the empty vector control (Fig. 5*C*). This activity demonstrates Ca^{2+} efflux *in vivo*, since only the inside-out vesicles can utilize the Mg-ATP required to drive the transport. To exclude the possibility that the difference observed was due either to variation in the stability of vesicles or to the amount of vesicles used, we performed a control experiment using leukotriene, which is glutathionated and taken up by ABCC-type transporters in yeast. We did not see any difference in leukotriene uptake activity between the two preparations (Fig. S8*B*). Concentration-dependent Ca^{2+} transport assays revealed that BjPCR1 is a high capacity and low affinity Ca^{2+} transporter exhibiting an apparent Km of 50 μM (Fig. S8*C*). To determine substrate specificity, competition of $^{45}Ca^{2+}$ transport assay was performed using cold Ca^{2+}, Fe^{2+} and Mn^{2+}. The $^{45}Ca^{2+}$ transport activity was inhibited by 93% and 38% by addition of Ca^{2+} and Mn^{2+} of 500 μM, but not by 500 μM Fe^{2+} (Fig. S8*D*). The result suggests that Ca^{2+} is a preferred substrate for BjPCR1 compared to other ions.

To determine how the BjPCR1-mediated Ca^{2+} transport was energized, we performed inhibitor studies (Fig. 5*D*). Vanadate, an inhibitor of P-type ATPases such as the plasma membrane proton pump, inhibited the transport by 80% compared to the Mg-ATP control, suggesting that the plasma membrane-localized H^+-ATPase generates the driving force for Ca^{2+} uptake. To test this hypothesis, we first examined the effect of ammonium chloride, which abolishes the ΔpH but not the membrane potential ($\Delta\psi_m$). In the presence of 5 mM ammonium chloride, Ca^{2+} transport was inhibited by 34%. This result indicated that BjPCR1 mediated Ca^{2+} uptake into yeast vesicles is partially ΔpH dependent, and that BjPCR1 does not act as a simple Ca^{2+} channel. To identify the additional driving force that supports the BjPCR1-mediated Ca^{2+} fluxes, we performed Ca^{2+} uptake experiments in the presence of valinomycin, which dissipates the $\Delta\psi_m$. In this case, Ca^{2+} transport was

inhibited by 51%, indicating that Ca^{2+} transport is electrogenic. Finally, the addition of carbonyl cyanide m-chlorophenylhydrate (CCCP), which disrupts both the ΔpH and $\Delta\psi_m$, had a drastic effect and inhibited Ca^{2+} transport activity by 99%. Two additional experiments provided further confirmation that the proton motive force drives BjPCR1-mediated Ca^{2+} transport: i) pre-incubation with Mg-ATP resulted in a faster Ca^{2+} uptake into yeast vesicles (Fig. S8*E*), and ii) yeast vesicles expressing BjPCR1 exhibited a more pronounced recovery of pH when challenged with Ca^{2+}, as indicated by the larger increase in 9-amino-6-chloro-2-methoxyacridine (ACMA) fluorescence in BjPCR1-expressing yeast microsomes than in EV-expressing ones (Fig. S8*F*). In this experiment, low pH-induced quenching of ACMA fluorescence was transiently reversed by the addition of Ca^{2+} to the medium, which is most likely due to H^+ release by Ca^{2+}/H^+ antiport activity. Together, these results indicate that Ca^{2+} transport by BjPCR1 is driven by a proton-coupled antiport mechanism. Since proton transport into vesicles by H^+-ATPase generates an inside-positive membrane potential, and a collapse of the membrane potential by valinomycin inhibited Ca^{2+} uptake into the vesicles, it is likely that more positive charges are exported than imported by BjPCR1 in the vesicle membrane (i.e., more charges carried by H^+ efflux than by Ca^{2+} influx, see below). This hypothesis is confirmed by a theoretical consideration, which, based on the following equation (for details see Supporting Materials and Methods),

$$E_{eq}^{exch} = \frac{1}{r-2}(rE_{H^+} - 2E_{Ca^{2+}}) \qquad (1)$$

where r is the stoichiometric coefficient of the exchange mechanism (rH$^+$:Ca^{2+}), and E_{H+} and E_{Ca2+} are the Nernst potential of H^+ and Ca^{2+}, respectively, shows that in the physiological ranges (shadowed area in Fig. S9*B*), the exchanger can always mediate Ca^{2+} efflux when one Ca^{2+} is exchanged with three protons.

Discussion

In this study, we demonstrated that *B. juncea* PCR1, a homologue of AtPCR2, exports Ca^{2+} from plant cells and acts as a Ca^{2+} transporter in plant protoplasts and membrane vesicles isolated from yeast cells. Arabidopsis Plant Cadmium Resistance (AtPCR) proteins 1 and 2 are small proteins that contain two predicted membrane-spanning α-helices, and contribute to Cd resistance and Zn homeostasis, respectively (11, 12). The PCR family of genes, characterized by the common

cysteine-rich PLAC8 domain, belongs to a large gene family that consists of many members in eukaryotes, including fungi, green algae, plants, and animals (16, 17). Two completely different functions have been associated with this gene family. On the one hand, the encoded proteins have been shown to act as transporters of Zn and Cd (11, 12); on the other, they have been associated with the control of the number of cells in fruits (16, 18).

Although *B. juncea* PCRs are highly similar in amino acid sequence to their Arabidopsis counterparts AtPCR1 and 2, antisense lines for *BjPCR1* were not compromised in zinc translocation, but, surprisingly, exhibited reduced translocation of Ca^{2+} to the shoot, which resulted in impaired growth. The impaired Ca^{2+} translocation into the shoot from the root of the *BjPCR1* antisense lines 5 and 17 is likely due to the impaired transfer of Ca^{2+} from the epidermal cells, where *BjPCR1* is highly expressed, to the inner cells of the root, as evidenced by the accumulation of fluo-3 signal at the root epidermis of the antisense lines (Fig. 2*F*). Interestingly, in Arabidopsis, the calcium concentration in roots seemed to be tightly controlled through Ca^{2+} translocation to the shoot, because Arabidopsis lines grown on low and high Ca^{2+} concentrations exhibited similar Ca^{2+} concentration in the roots, whereas the shoots of plants grown on higher Ca^{2+} concentrations contained higher Ca^{2+} concentrations than those grown on lower Ca^{2+} concentrations (Fig. S7*D*). Thus, under high Ca^{2+} concentration conditions, Arabidopis plants expressing *BjPCR1* in the epidermis translocated more calcium from the root to the shoot, which contributed to their improved calcium tolerance (Fig. 4), most likely due to dilution effect. Together, these results indicate that the extrusion of Ca^{2+} by BjPCR1 from the epidermal cells to the apoplast of the cortical layer of the root is required for the efficient movement of Ca^{2+} from the root to the shoot. In addition, our temperature-dependent Ca^{2+} transport assay (Fig. S6) revealed that the antisense BjPCR1 plants retained more Ca^{2+} in the root than the wild type, indicating that the energy-dependent activity of BjPCR1 is responsible for the removal of $Ca^{2+}$from the root. Since there is no extensive symplastic connection via plasmodesmata between the epidermal and cortical layers of cells in the root (19, 20), BjPCR1 is expected to remove Ca^{2+} to the apoplast of the root, and thereby contributes to the translocation of Ca^{2+} from the root to the shoot. There is some debate on whether Ca^{2+} is delivered to the xylem by the apoplastic or symplastic pathway across the endodermal layer of the root (1, 8, 21, 22). So far, the available data indicate that

Ca^{2+} uptake and transfer to the xylem are achieved by a complex mechanism, which is highly regulated and may differ from one plant to another. However, at least in *B. juncea*, it is clear from our results that apoplastic transfer of Ca^{2+} at the interface of epidermal/cortical cells is an important step in the radial transfer of Ca^{2+} across the root. A similar function in radial translocation of metal ions at the root epidermis has been described for AtPCR2 (12). AtPCR2 is a zinc efflux transporter located at the plasma membrane of root xylem cells and epidermal cells, and an atpcr2 knockout mutant exhibited reduced zinc translocation to shoots. Thus, efflux transport systems may be required for the radial transfer of mineral ions from epidermal to inner layers through the apoplastic pathway.

No transporter has yet been shown to be responsible for the radial transport of Ca^{2+} in the root. Plant roots need to transport high levels of Ca^{2+} in a radial direction from the epidermis to the vascular tissue, since shoots require a large amount of Ca^{2+} (4). To translocate high levels of Ca^{2+} through the epidermal cells to the inner part of a root, a high capacity Ca^{2+} transporter, such as a plasma membrane-localized H^+/Ca^{2+} or Na^+/Ca^{2+} antiporter, has been postulated to exist, because epidermal cells do not contain enough plasmadesmata for an efficient symplasmic transfer of Ca^{2+}. In mammals, a Na^+/Ca^{2+} exchanger (NCX) prevents significant increases in intracellular Ca^{2+} by exhibiting a low-affinity and high-capacity efflux activity (23). In plants, the presence of plasma membrane-localized H^+/Ca^{2+} antiporters was suggested based on a biochemical assay that used plasma membrane-derived vesicles from *Zea mays* (corn) leaves and roots; however, no plasma membrane-localized H^+/Ca^{2+} antiporter gene has yet been reported in plant (6, 7). Ca^{2+} transport assays using BjPCR1-expressing yeast vesicles imply that BjPCR1 can function as a high capacity, low affinity H^+/Ca^{2+} exporter. Experiments with agents abolishing either the ΔpH, the $\Delta\Psi$ or both, together with theoretical considerations revealed that, using a stoichiometry of at least three protons per exported Ca^{2+}, BjPCR1 can efficiently export Ca^{2+} from the cell. A mammalian Na^+/Ca^{2+} antiporter (NCX) (24, 25) has a stoichiometry of 3 or $4Na^+:Ca^{2+}$, while for a vacuolar Ca^{2+} proton antiporter a stoichiometry of 3 H^+ per Ca^{2+} has been postulated (26). Furthermore, studies of a H^+/Ca^{2+} antiporter from *Escherichia coli* also pointed to a stoichiometry of higher than $2H^+:Ca^{2+}$ (27).

Although Ca^{2+} is available in sufficient amounts in the soil, Ca-related disorders, such as bitter pit in apple fruit, blossom-end rot in tomato fruit, and tip burn in the

leaves of vegetables, can occur, especially in vigorously growing plants and in parts of the plant that demand a high level of Ca^{2+}. It is therefore likely that these plants are limited in their ability to transfer Ca^{2+} to the above-ground parts, and that genetically engineering crops with BjPCR1 might improve the quality and yield of these plants.

Besides acting as cation transporters, members of the PLAC8 motif-containing family have been associated with the control of cell number (16, 18). Therefore, it remains an open question as to whether other genes that contain the common PLAC8 motif regulate cell number through the transport of divalent cations, in a manner similar to other members of the PCR family. The fact that PCRs act as transporters of the classical signaling compound Ca^{2+} (in the case of BjPCR1) and the important enzyme cofactor Zn^{2+} (in the case of AtPCR2) may indicate that cell number is also adjusted by the transport of such cations.

Materials and Methods

Plant growth conditions and Ca translocation experiment

The *Brassica juncea* 182921 line (28) was grown on rock-wool block containing hydroponic nutrient solution (see SI Materials and Methods). For the $^{45}CaCl_2$ uptake experiment, anti-BjPCR1 lines and wild-type *B. juncea* plants were grown in half-strength hydroponic medium for three weeks. Then, the plants were incubated in hydroponic nutrient solution supplemented with 0.4 MBq $^{45}CaCl_2$ for 5 and 12 h, and shoots were separated from the roots. The radioactivity was measured using a liquid scintillation counter (Perkin Elmer). Autoradiography of $^{45}CaCl_2$ was performed on plants incubated in medium supplemented with 0.4 MBq $^{45}CaCl_2$ for 12 h.

Supporting information. For other methods, see SI Materials and Methods.

Acknowledgements

This work was supported by grants from the Global Research Laboratory program of the Ministry of Education, Science and Technology (MEST) of Korea (K20607000006), awarded to Y. L. and E. M., the World Class University (WCU) program through the National Research Foundation of Korea funded by the MEST

(R31-10105), and Cooperative Research Program of Rural Development Administration (PJ0074482011), to Y.L., the EU project PHIME (FOOD-CT-2006-0016253), awarded to E.M., and an EMBO fellowship to A.D.A. (ALTF 872009). We would like to thank Dr. Armando Carpaneto for performing the oocyte experiments and Prof. Ueli Grossniklaus for the help in initial in situ hybridization experiments.

References

1. Marschner H (1995). *Mineral Nutrition of Higher Plants*. Academic Press, San Diego.
2. White PJ & Broadley MR (2003) Calcium in plants. *Ann Bot* 92: 487-511.
3. Maathuis FJM (2009) Physiological functions of mineral macronutrients. *Curr Opin Plant Biol* 12: 250-258.
4. White PJ *et al*. (2002) Genes for calcium-permeable channels in the plasma membrane of plant root cells. *Biochim Biophys Acta* 1564: 299-309.
5. Kudla J, Batistič O & Hashimoto K (2010) Calcium Signals: The lead currency of plant information processing. *Plant Cell* 22: 541-563.
6. Kasai M & Muto S. (1990) Ca^{2+} pump and Ca^{2+}/H^{+} antiporter in plasma membrane vesicles isolated by aqueous two phase partitioning from corn leaves. *J Membr Biol* 114: 133-142.
7. Vicente JAF & Vale MGP (1995) Activities of Ca^{2+} pump and low affinity Ca^{2+}/H^{+} antiport in plasma membrane vesicles of corn roots. *J Exp Bot* 46:1551-1559.
8. White PJ (2001) The pathways of calcium movement to the xylem. *J Exp Bot* 52: 891-899.
9. Cholewa E & Peterson CA (2004) Evidence for symplastic involvement in the radial movement of calcium in onion roots. *Plant Physiol* 134: 1793-1802.
10. Hayter ML & Peterson CA (2004) Can Ca^{2+} fluxes to the root xylem be sustained by Ca^{2+}-ATPases in exodermal and endodermal plasma membranes? *Plant Physiol* 136: 4318-4325.
11. Song WY *et al*. (2004). A novel family of cys-rich membrane proteins mediates cadmium resistance in Arabidopsis. *Plant Physiol* 135: 1027-1039.
12. Song WY *et al*. (2010) Arabidopsis PCR2 is a zinc exporter Involved in both zinc extrusion and long-distance zinc transport. *Plant Cell* 22: 2237-2252.

13. Zhang WH, Rengel Z, Kuo J(1998) Determination of intracellular Ca^{2+} in cells of intact wheat roots: loading of acetoxymethyl ester of Fluo-3 under low temperature. *Plant J* 15:147–151.
14. Cho HT & Cosgrove DJ (2002) Regulation of root hair initiation and expansin gene expression in Arabidopsis. *Plant Cell* 14: 3237–3253.
15. Hussain D *et al*. (2004) P-type ATPase heavy metal transporters with roles in essential zinc homeostasis in Arabidopsis. *Plant Cell* 16: 1327-1339.
16. Guo M *et al*. (2010). Cell Number Regulator1 affects plant and organ size in maize: implications for crop yield enhancement and heterosis. *Plant Cell 22*: 1057-1073.
17. Song WY *et al*. (2011) Common functions or only phylogenetically related? The large family of PLAC8 motif-containing/PCR genes. *Mol & Cells* 31: 1-7.
18. Frary *et al*. (2000) fw2.2: A quantitative trait locus key to the evolution of tomato fruit size. *Science* 289: 85-88.
19. Zhu T, Lucas WJ & Rost TL (1998) Directional cell-to-cell communication in the Arabidopsis root apical meristem I. An ultrastructural and functional analysis. *Protoplasma* 203: 35-47.
20. Ma F & Peterson CA (2001) Frequencies of plasmodesmata in Allium cepa L. roots: implications for solute transport pathways. *J Exp Bot* 52: 1051-1061.
21. McLaughlin SB & Wimmer R (1999). Calcium physiology and terrestrial ecosystem processes. *New Phytology* 142: 373-417.
22. Yang HQ, Jie YL, Zhang LZ & Cui MG (2004) The effect of IBA on the Ca^{2+} absorption and Ca^{2+}-ATPase activity and their ultracytochemical localization in apple roots. *Acta Hort* 636: 211-219.
23. Noble D & Herchuelz A (2007) Role of Na/Ca exchange and the plasma membrane Ca^{2+}-ATPase in cell function. *EMBO reports* 8: 228 - 232.
24. Fujioka Y, Hiroe K & Matsuoka S (2000) Regulation kinetics of Na^{+}-Ca^{2+} exchange current in guinea-pig ventricular myocytes. *J Physiol* 529: 611-623.
25. Dong H, Dunn J & Lytton J (2002). Stoichiometry of the Cardiac Na^{+}/Ca^{2+} exchanger NCX1.1 measured in transfected HEK cells. *Biophys J* 82: 1943-1952.
26. Brey RN, Rosen BP & Sorensen EN (1980) *Cation/proton antiport systems in Escherichia coli*. Properties of the potassium/proton antiporter. *J Biol Chem* 255: 39-44.

27. Blackford S, Rea PA & Sanders D (1990) Voltage sensitivity of H^+/Ca^{2+} antiport in higher plant tonoplast suggests a role in vacuolar calcium accumulation. *J Biol Chem* 265: 9617-9620.
28. Ebbs SD & Kochian LV (1998) Phytoextraction of zinc by oat (*Avena sativa*), barley (*Hordeum vulgare*), and Indian mustard (*Brassica juncea*). *Environ Sci and Technol* 32: 802-806.

Figure legends

Figure 1. Characterization of BjPCR1.

(A) Comparison of PCRs of *A. thaliana* and *B. juncea* by amino acid sequence alignment. Identical or similar amino acid residues are in black or gray boxes. ClustalW was used to generate the alignment. (B-D) Phenotype analysis of *BjPCR1* knock-down mutants. (B)Transcription levels of *BjPCR1* in wild-type and anti-BjPCR1 *B. juncea* (lines 4, 5, 8, 16, and 17) plants. (C) Growth of two-week-old wild-type (WT) and anti-BjPCR1 (lines 5, 8, 17) plants in hydroponic culture. (D) Fresh weight of the shoots and roots of wt and anti-BjPCR1 (lines 5, 8, 17) plants grown as shown in C. The average ±SE is shown (n=20, N=3).

Figure 2. The *BjPCR1* antisense lines exhibited reduced translocation of Ca^{2+} to the shoot and reduced radial translocation of Ca^{2+} to the inner part of the root.

(A) Ca and (B) Zn concentrations in the shoots and roots of four-week-old wild-type (WT) and anti-BjPCR1 *B. juncea* plants. (C) Shoot to root ratios of Ca and Zn concentrations as shown in (A) and (B). (D) Autoradiography of three-week-old *B. juncea* plants incubated in hydroponic medium supplemented with 1.5 mM $CaCl_2$ containing 0.4 MBq $^{45}CaCl_2$ supplied through the root for 15 h. (E) Counts of ^{45}Ca normalized by the volume of cell sap extracted from the shoot of plants treated with $^{45}CaCl_2$ as in (D). All data represent average ± SE (*n* = 5, N=2). (F) Distribution of free Ca^{2+} in the roots of the wild type (WT) and anti-BjPCR1 lines, visualized using fluo-3 fluorescence. Roots of five-day-old *B. juncea* plants were stained with fluo-3 for 4 h, washed with PBS solution, and observed by confocal microscopy. Bars= 500 μm.

Figure 3. Expression pattern and subcellular localization of BjPCR1.

(A) RT-PCR analysis of *BjPCR1* and *BjPCR2* in *B. juncea* plants. (B) Localization of *BjPCR1* and *BjPCR2* transcripts in the roots of B. *juncea* grown on agar medium for five days. *BjEXP7* and *BjHMA4* were used as marker genes that are expressed in root hairs and vascular tissue, respectively. Root cell layers were collected in liquid nitrogen, sequentially ground four times, and collected, and their mRNA was extracted as described in Supporting Materials and Methods. (C) Localization of *BjPCR1* in the roots of *B. juncea*, as detected by the whole mount *in situ* RNA hybridization technique, using a fluorescein-12-UTP labeled-antisense (left) or -sense (right; background control) probe. Optically sectioned images of the median planes of the samples were obtained by confocal microscopy. Bar= 500 μm. (D) Expression pattern of *BjPCR1* and *BjPCR2* under excess (10 mM $CaCl_2$) and deficient (0 mM $CaCl_2$) calcium conditions. The average ±SE is shown (*n=3*, *N=2*). (E, F) Plasma membrane localization of BjPCR1-GFP. (E) Fluorescence at the root epidermis of a BjPCR1-GFP transgenic Arabidopsis plant. The red fluorescence indicates the vacuoles and endosomes stained with FM4-64. (F) Fluorescence of BjPCR1-GFP at the leaf epidermis of a BjPCR1-GFP-expressing tobacco plant. Red fluorescence indicates the cell walls and nuclei of epidermal cells stained with propidium iodide. Left, bright field images; middle, merged images of red fluorescence and green fluorescence; right, images enlarged from the boxed areas in the first two columns. Bar= 5 μm.

Figure 4. Arabidopsis lines expressing *BjPCR1* in root hairs exhibited enhanced calcium resistance and translocation to the shoot.

(A) Root hair-specific localization of *BjPCR1* in *EXP7promoter::BjPCR1-GFP* transgenic Arabidopsis. Bar = 5 μm. (B) The calcium tolerance phenotype of *EXP7promoter::BjPCR1* transgenic Arabidopsis lines (EXP7p::BjPCR1-1 and -2). Plants were grown on 30 mM $CaCl_2$ containing 1/2 MS medium for 3 weeks. (C) Shoot to root calcium ratio in *EXP7promoter::BjPCR1*-expressing Arabidopsis lines (BjPCR1-1 and -2). Calcium content was measured and the shoot to root calcium ratio was analyzed using data from Fig. S7*C*. Average values ±SE are shown (n=3, N=2).

Figure 5. Ca^{2+} transport mediated by BjPCR1.

(A) Time-dependent Ca^{2+} uptake by protoplasts of wild-type and anti-BiPCR1-5 and -17 *B. juncea*. The protoplasts were suspended in loading buffer containing 100 μM $CaCl_2$, 18.5 kBq $^{45}CaCl_2$, and 18.5 kBq $^{3}H_2O$, and incubated for the indicated periods of time. Only the intact protoplasts were collected by centrifugation. (B) Time-dependent release of Ca^{2+} from protoplasts of wild-type and anti-BjPCR1 plants. The protoplasts were pre-loaded in medium containing 100 μM $CaCl_2$ and 18.5 kBq $^{45}CaCl_2$ for 30 min, washed briefly with ice-cold bathing solution, and incubated in the bathing medium. Only intact cells were collected and radioactive disintegrations from the samples were counted. The Ca^{2+} content was normalized against the $^{3}H_2O$ content of the protoplasts. The average ± SE are shown (n=4, N=3). (C, D) Ca^{2+} uptake experiment in yeast microsomes isolated from *Saccharomyces cerevisiae* transformed with the empty vector (V) or BjPCR1 (BP1). (C) Time course of Ca^{2+} uptake by vesicles from cells transformed with V or BP1. Ca^{2+} uptake was performed in the absence (-ATP) or presence (+ATP) of 4 mM Mg-ATP in Ca transport medium containing a standard transport buffer at 25ºC for the indicated period of time. The microsomes were collected by filtration on a nitrocellulose filter. (D) Effects of inhibitors of ion transport on Ca^{2+} uptake by vesicles derived from BjPCR1 (BP1)-expressing cells. Uptake assay was performed using yeast microsomes expressing empty vector (V) or BjPCR1 (BP1) in the Ca^{2+} transport medium containing 4 mM Mg-ATP (Control) plus the compounds indicated (i.e., NH_4Cl, 5 mM; vanadate, 1 mM; valinomycin, 2 μM; and CCCP, 10 μM). The bars represent the Ca^{2+} concentrations in vesicles expressing BjPCR1 minus those in vesicles transformed with empty vector (n=4, N=2). The values (%) in the graph are the rates of uptake expressed as a percentage of the control. Average values ±SE are shown (n=3, N=2).

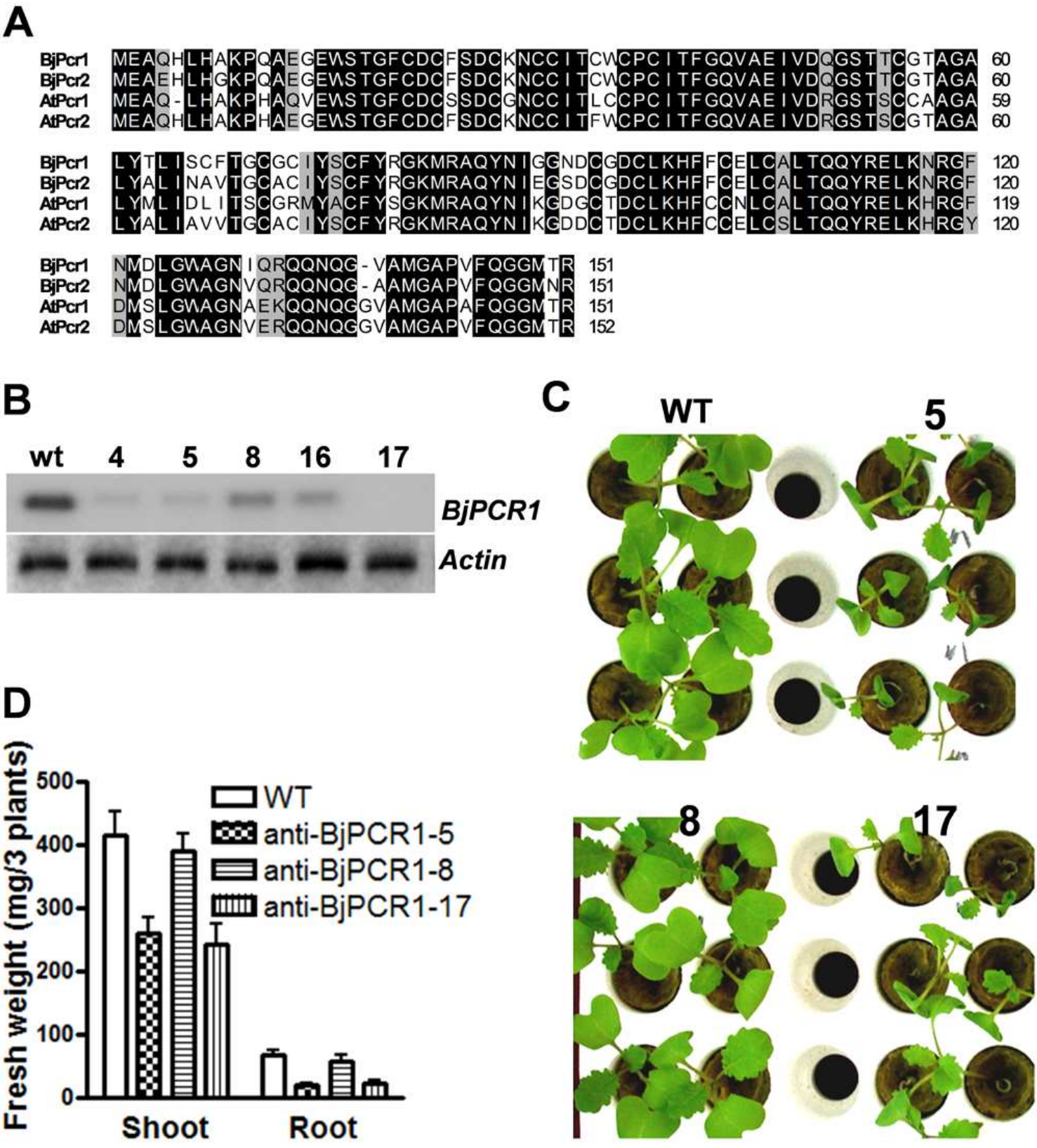
A
BjPcr1 MEAQHLHAKPQAEGEWSTGFCDCFSDCKNCCITCWCPCITFGQVAEIVDQGSTTCGTAGA 60
BjPcr2 MEAEHLHGKPQAEGEWSTGFCDCFSDCKNCCITCWCPCITFGQVAEIVDQGSTTCGTAGA 60
AtPcr1 MEAQ-LHAKPHAQVEWSTGFCDCSSDCGNCCITLCCPCITFGQVAEIVDRGSTSCCAAGA 59
AtPcr2 MEAQHLHAKPHAEGEWSTGFCDCFSDCKNCCITFWCPCITFGQVAEIVDRGSTSCGTAGA 60
BjPcr1 LYTLISCFTGCGCIYSCFYRGKMRAQYNIGGNDCGDCLKHFFCELCALTQQYRELKNRGF 120
BjPcr2 LYALINAVTGCACIYSCFYRGKMRAQYNIEGSDCGDCLKHFFCELCALTQQYRELKNRGF 120
AtPcr1 LYMLIDLITSCGRMYACFYSGKMRAQYNIKGDGCTDCLKHFCCNLCALTQQYRELKHRGF 119
AtPcr2 LYALIAVVTGCACIYSCFYRGKMRAQYNIKGDDCTDCLKHFCCELCSLTQQYRELKHRGY 120
BjPcr1 NMDLGWAGNIQRQQNQG-VAMGAPVFQGGMTR 151
BjPcr2 NMDLGWAGNVQRQQNQG-AAMGAPVFQGGMNR 151
AtPcr1 DMSLGWAGNAEKQQNQGGVAMGAPAFQGGMTR 151
AtPcr2 DMSLGWAGNVERQQNQGGVAMGAPVFQGGMTR 152
B
wt 4 5 8 16 17
BjPCR1
Actin
C
WT
5
8
17
D
Fresh weight (mg/3 plants)
500
400
300
200
100
0
WT
anti-BjPCR1-5
anti-BjPCR1-8
anti-BjPCR1-17
Shoot
Root

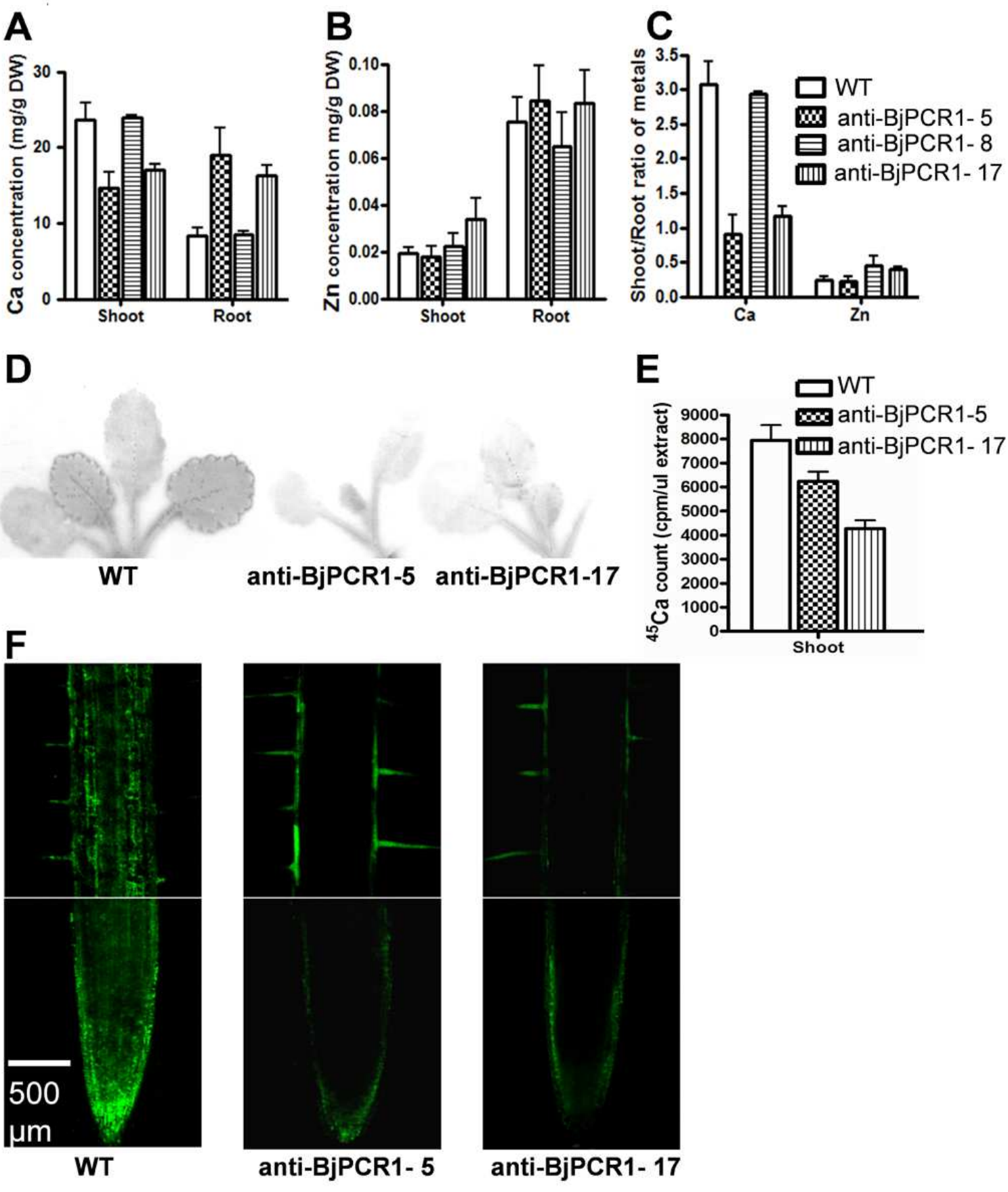
A
Ca concentration (mg/g DW)
30
20
10
0
Shoot
Root
B
Zn concentration mg/g DW)
0.10
0.08
0.06
0.04
0.02
0.00
Shoot
Root
C
Shoot/Root ratio of metals
3.5
3.0
2.5
2.0
1.5
1.0
0.5
0.0
Ca
Zn
WT
anti-BjPCR1- 5
anti-BjPCR1- 8
anti-BjPCR1- 17
D
WT
anti-BjPCR1-5
anti-BjPCR1-17
E
WT
anti-BjPCR1-5
anti-BjPCR1- 17
45Ca count (cpm/ul extract)
9000
8000
7000
6000
5000
4000
3000
2000
1000
0
Shoot
F
500
μm
WT
anti-BjPCR1- 5
anti-BjPCR1- 17

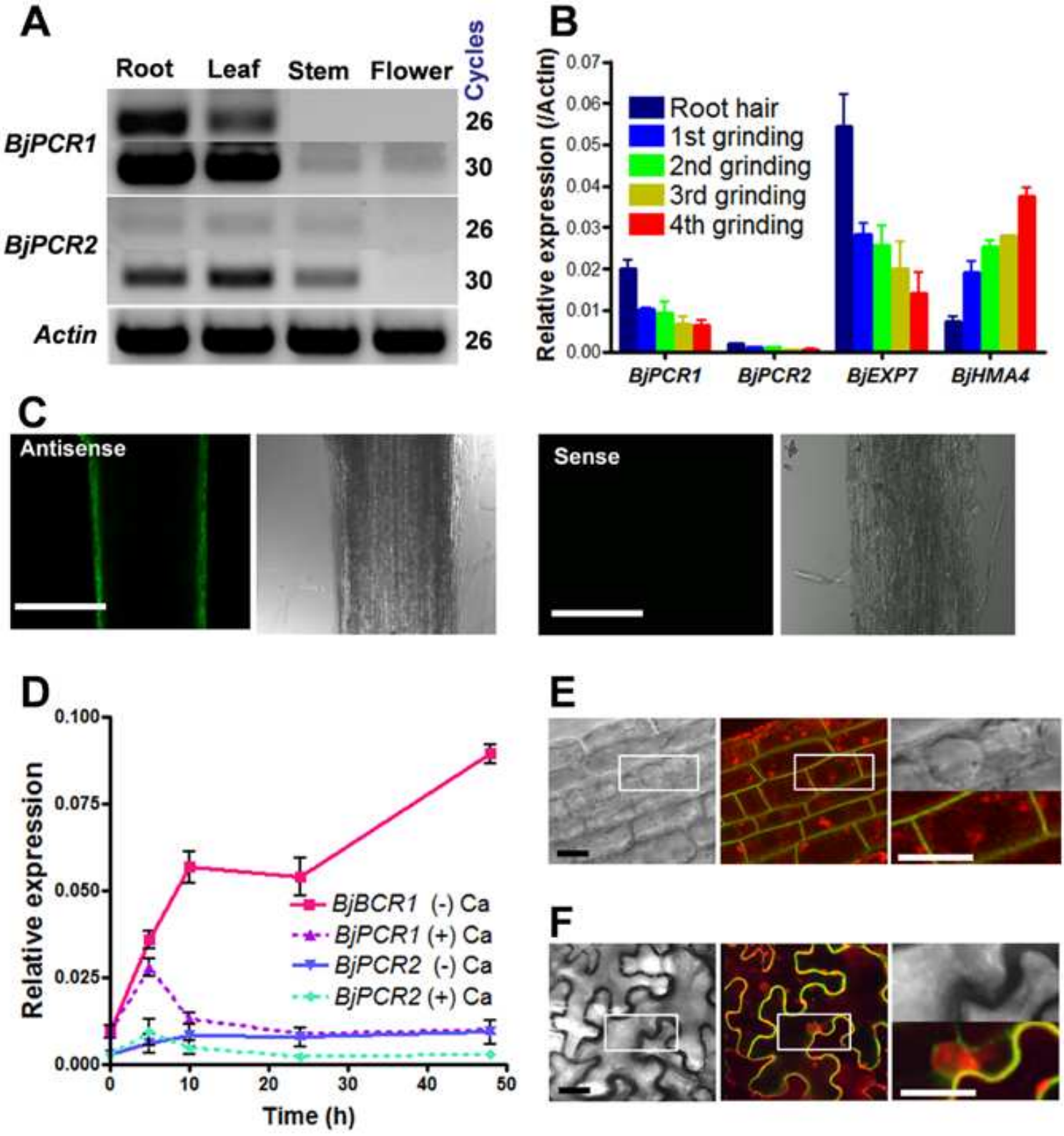
A
Root
Leaf
Stem
Flower
Cycles
BjPCR1
26
30
BjPCR2
26
30
Actin
26
B
Relative expression (/Actin)
0.07
0.06
0.05
0.04
0.03
0.02
0.01
0.00
Root hair
1st grinding
2nd grinding
3rd grinding
4th grinding
BjPCR1
BjPCR2
BjEXP7
BjHMA4
C
Antisense
Sense
D
Relative expression
0.100
0.075
0.050
0.025
0.000
0
10
20
30
40
50
Time (h)
BjBCR1 (-) Ca
BjPCR1 (+) Ca
BjPCR2 (-) Ca
BjPCR2 (+) Ca
E
F

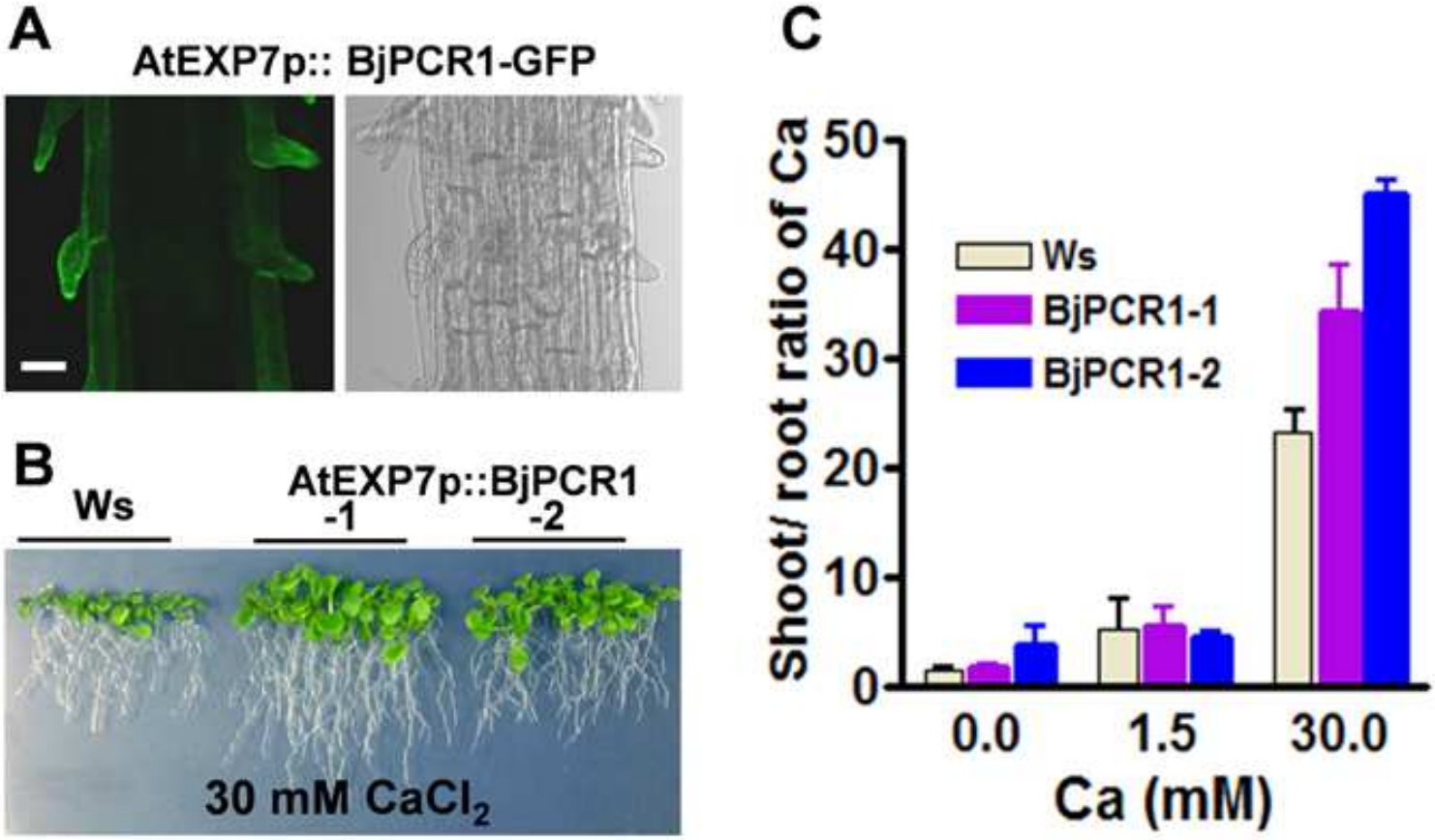
A
AtEXP7p:: BjPCR1-GFP
B
Ws
AtEXP7p::BjPCR1
-1
-2
30 mM CaCl2
C
Shoot/ root ratio of Ca
50
40
30
20
10
0
Ws
BjPCR1-1
BjPCR1-2
0.0
1.5
30.0
Ca (mM)

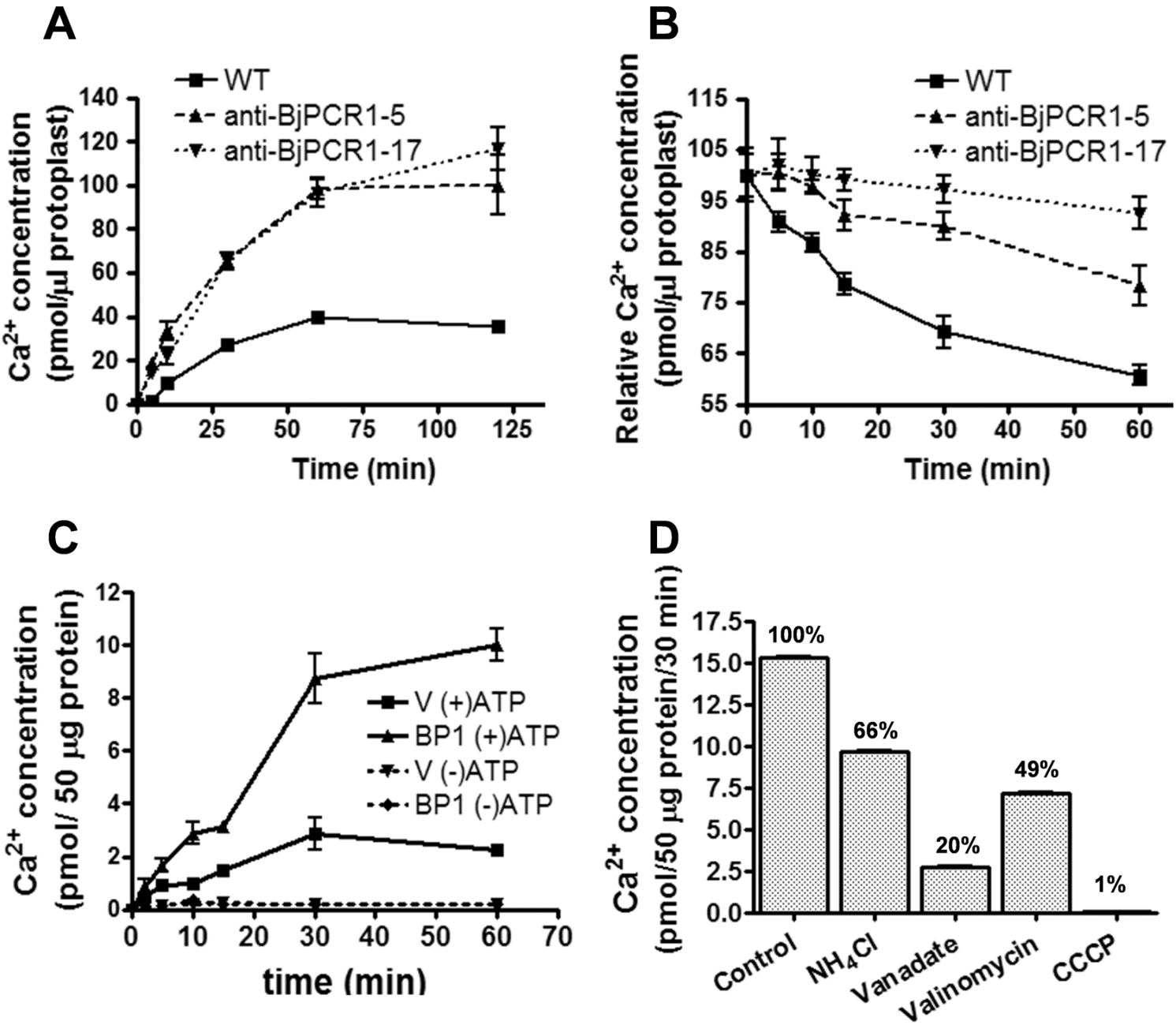
A
WT
anti-BjPCR1-5
anti-BjPCR1-17
Ca2+ concentration (pmol/µl protoplast)
Time (min)
B
WT
anti-BjPCR1-5
anti-BjPCR1-17
Relative Ca2+ concentration (pmol/µl protoplast)
Time (min)
C
V (+)ATP
BP1 (+)ATP
V (-)ATP
BP1 (-)ATP
Ca2+ concentration (pmol/ 50 µg protein)
time (min)
D
Ca2+ concentration (pmol/50 µg protein/30 min)
100%
66%
20%
49%
1%
Control
NH4Cl
Vanadate
Valinomycin
CCCP

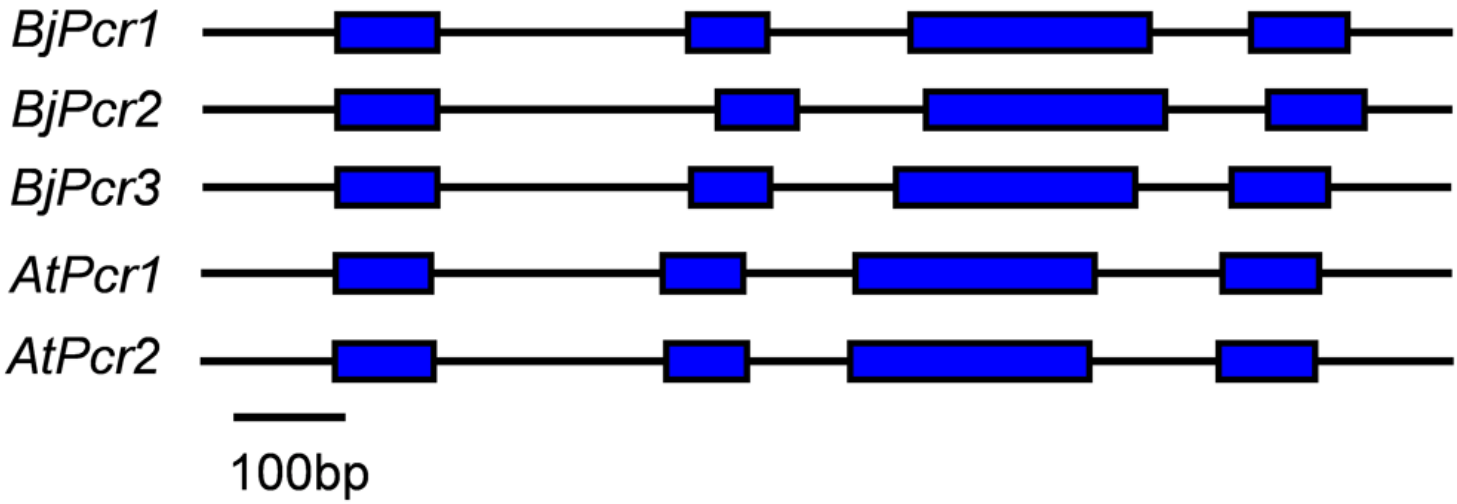
BjPcr1
BjPcr2
BjPcr3
AtPcr1
AtPcr2
100bp

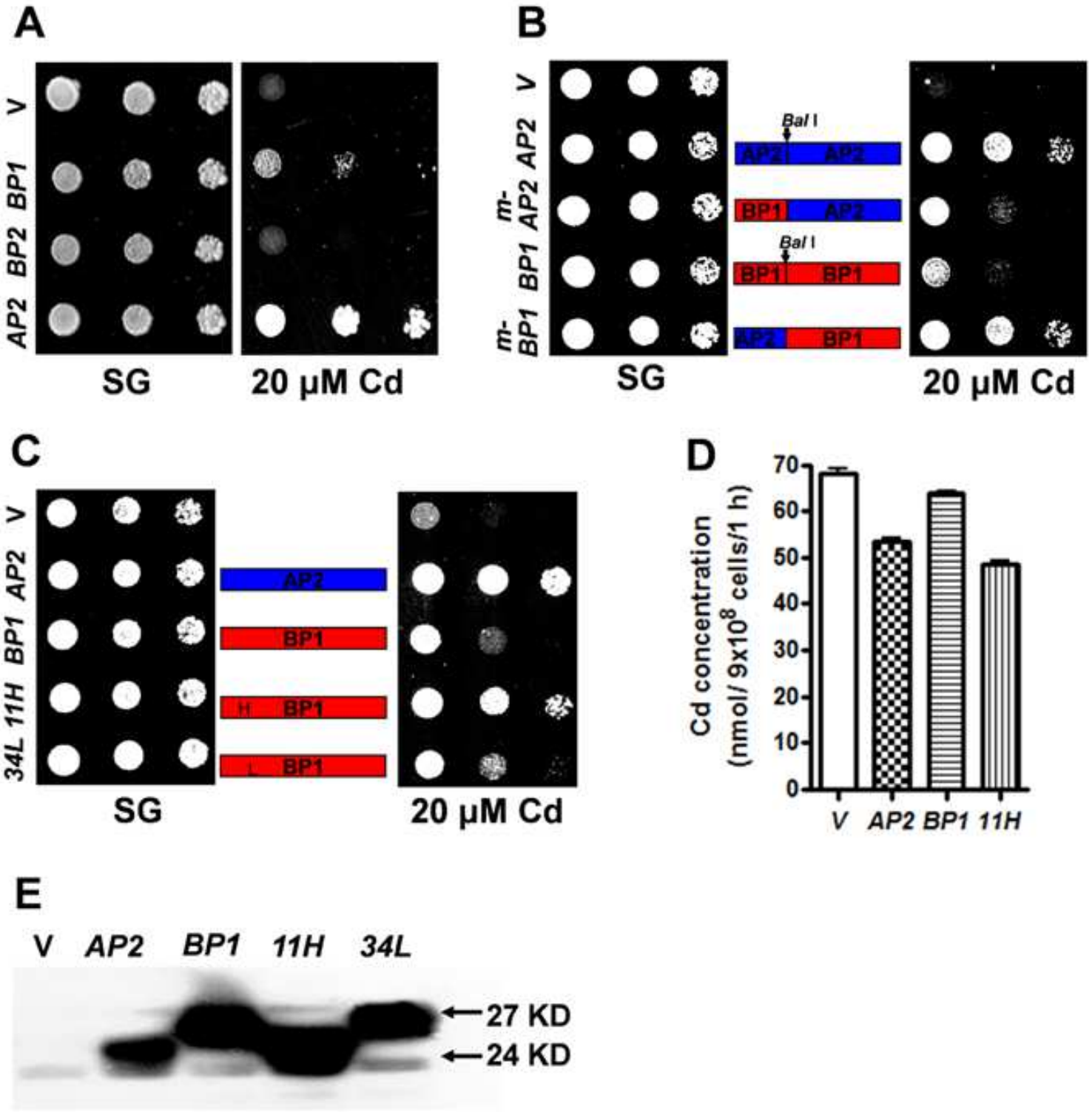
A
V
BP1
BP2
AP2
SG
20 μM Cd
B
V
m-AP2
m-BP1
Bal I
AP2
BP1
SG
20 μM Cd
C
V
AP2
BP1
11H
34L
H
L
SG
20 μM Cd
D
Cd concentration (nmol/ 9x10^8 cells/1 h)
70
60
50
40
30
20
10
0
V
AP2
BP1
11H
E
V
AP2
BP1
11H
34L
27 KD
24 KD

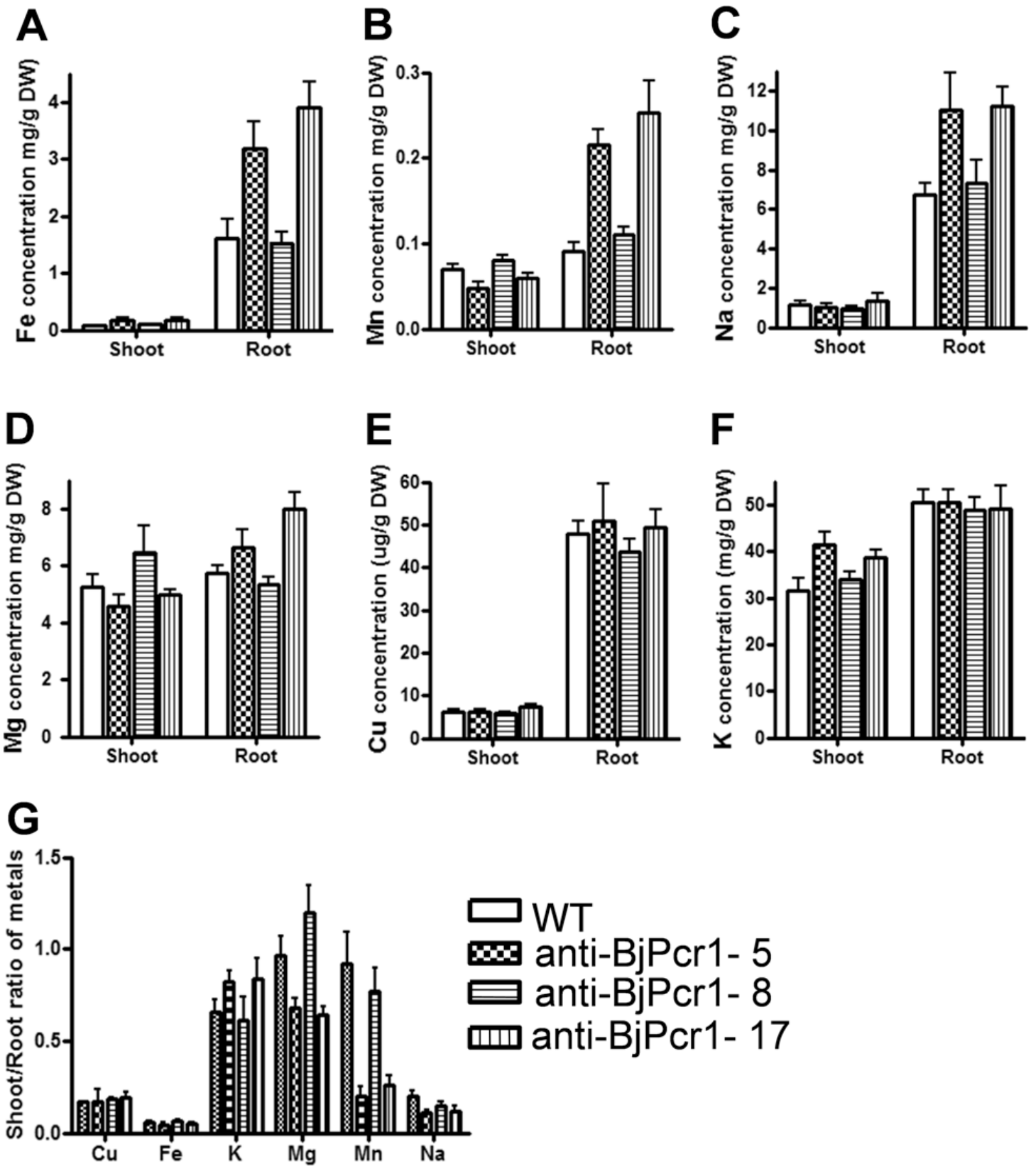
A
Fe concentration mg/g DW)
0
1
2
3
4
Shoot
Root
B
Mn concentration mg/g DW)
0.0
0.1
0.2
0.3
Shoot
Root
C
Na concentration mg/g DW)
0
2
4
6
8
10
12
Shoot
Root
D
Mg concentration mg/g DW)
0
2
4
6
8
Shoot
Root
E
Cu concentration (ug/g DW)
0
10
20
30
40
50
60
Shoot
Root
F
K concentration (mg/g DW)
0
10
20
30
40
50
Shoot
Root
G
Shoot/Root ratio of metals
0.0
0.5
1.0
1.5
Cu
Fe
K
Mg
Mn
Na
WT
anti-BjPcr1- 5
anti-BjPcr1- 8
anti-BjPcr1- 17

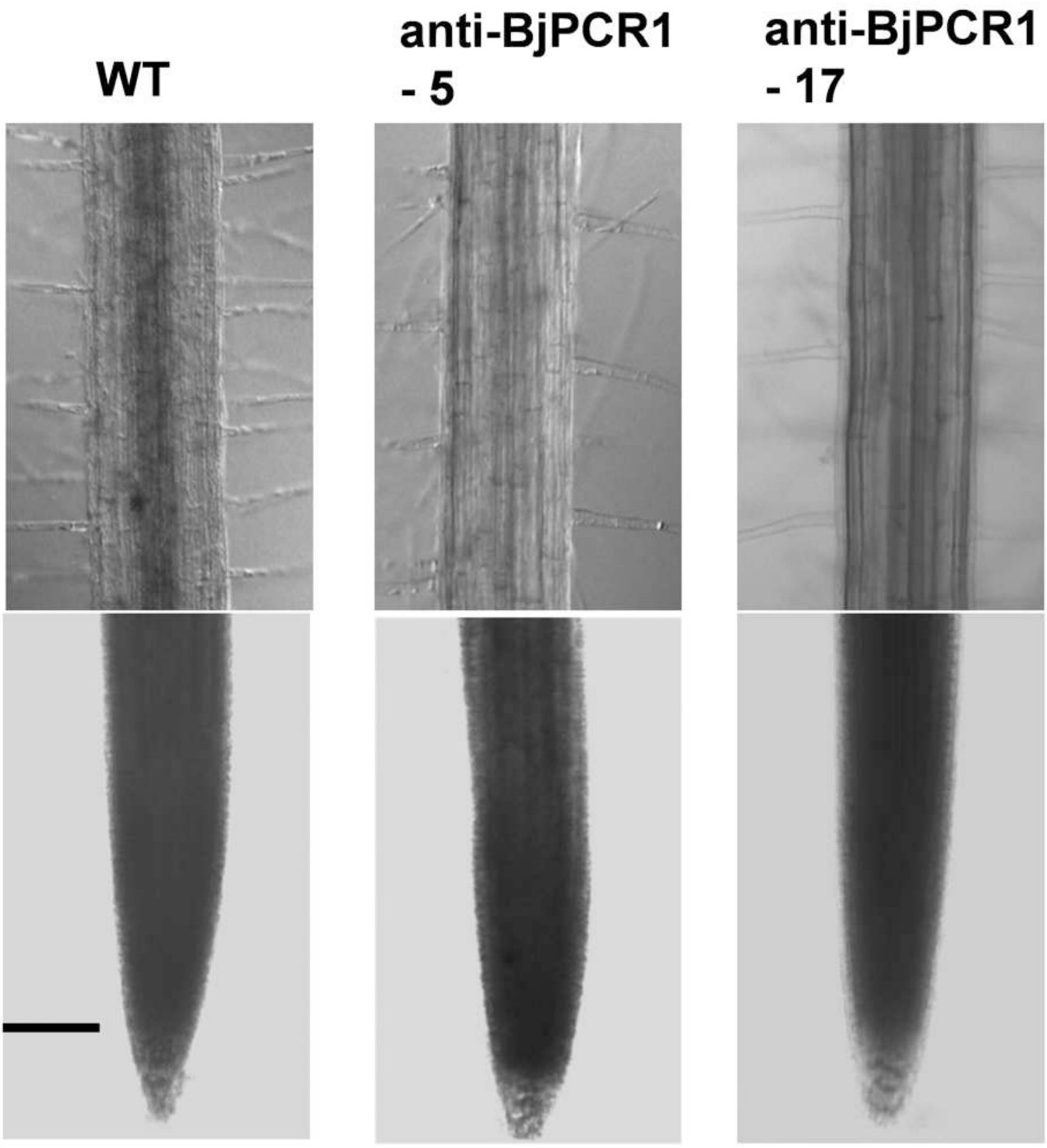
WT
anti-BjPCR1 - 5
anti-BjPCR1 - 17

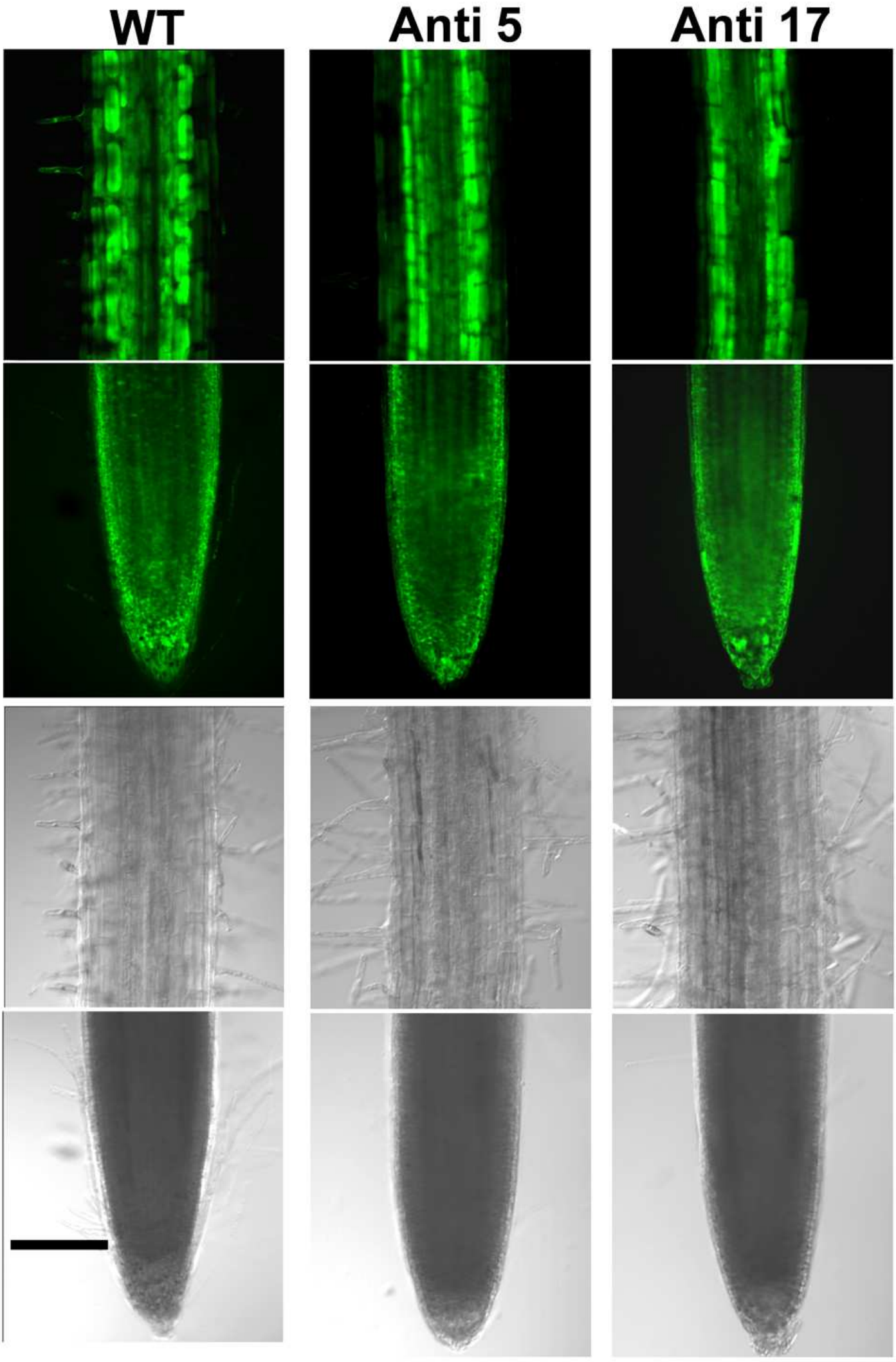
WT
Anti 5
Anti 17

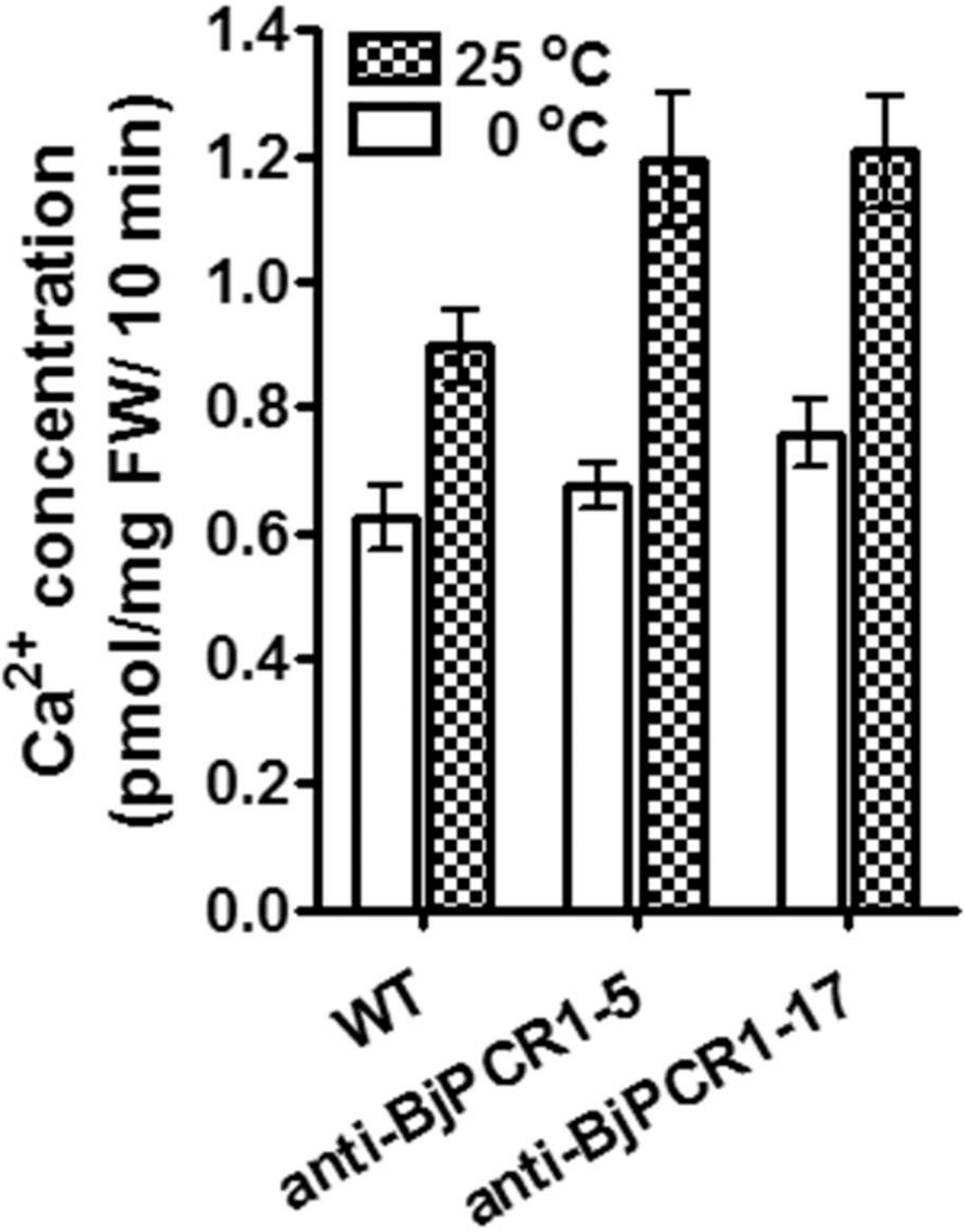
25 °C
0 °C
1.4
1.2
1.0
0.8
0.6
0.4
0.2
0.0
Ca2+ concentration
(pmol/mg FW/ 10 min)
WT
anti-BjP CR1-5
anti-BjP CR1-17

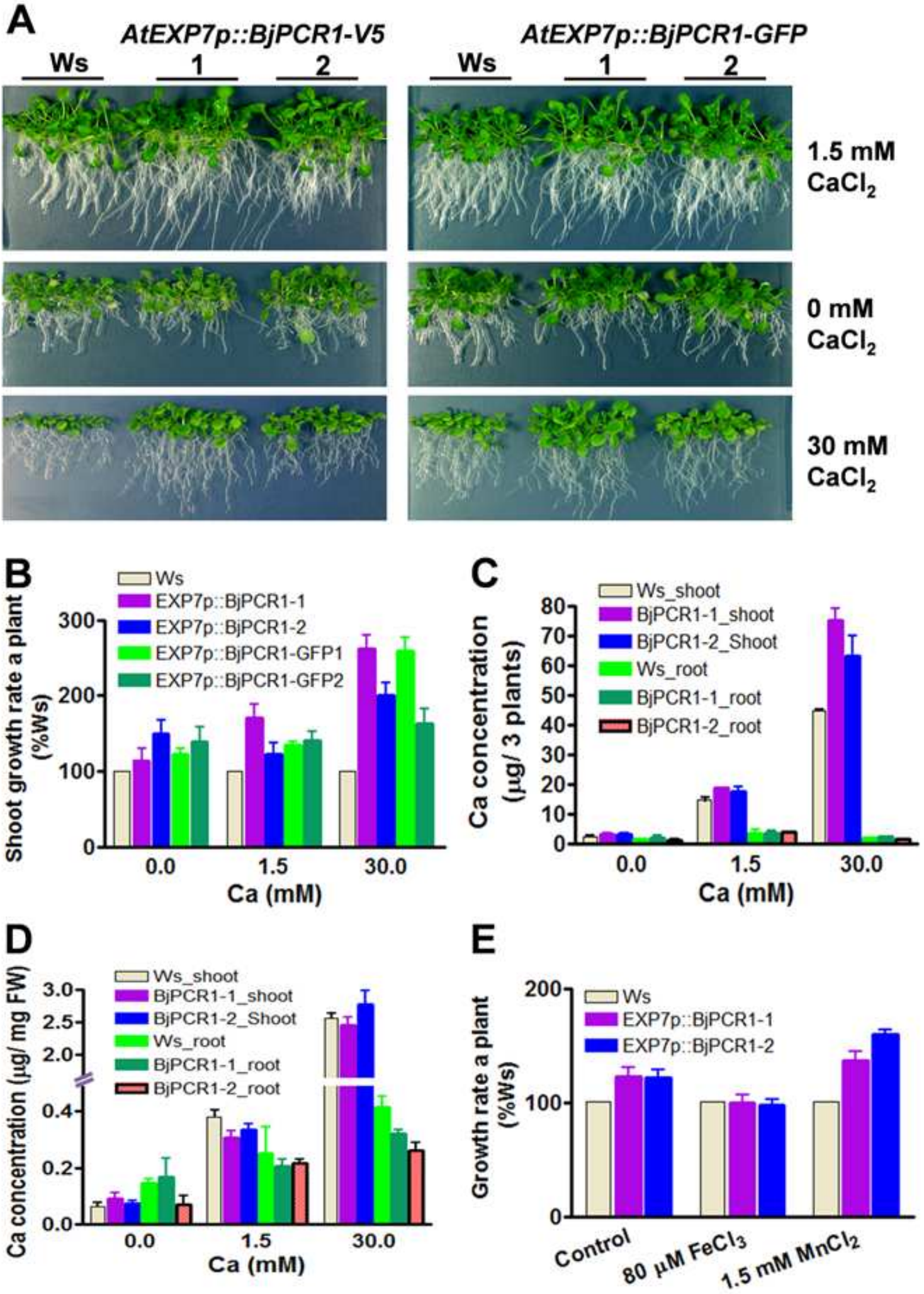
A
AtEXP7p::BjPCR1-V5
AtEXP7p::BjPCR1-GFP
Ws
1
2
1.5 mM CaCl2
0 mM CaCl2
30 mM CaCl2
B
Ws
EXP7p::BjPCR1-1
EXP7p::BjPCR1-2
EXP7p::BjPCR1-GFP1
EXP7p::BjPCR1-GFP2
Shoot growth rate a plant (%Ws)
Ca (mM)
C
Ws_shoot
BjPCR1-1_shoot
BjPCR1-2_Shoot
Ws_root
BjPCR1-1_root
BjPCR1-2_root
Ca concentration (µg/ 3 plants)
Ca (mM)
D
Ca concentration (µg/ mg FW)
Ca (mM)
E
Growth rate a plant (%Ws)
Control
80 µM FeCl3
1.5 mM MnCl2

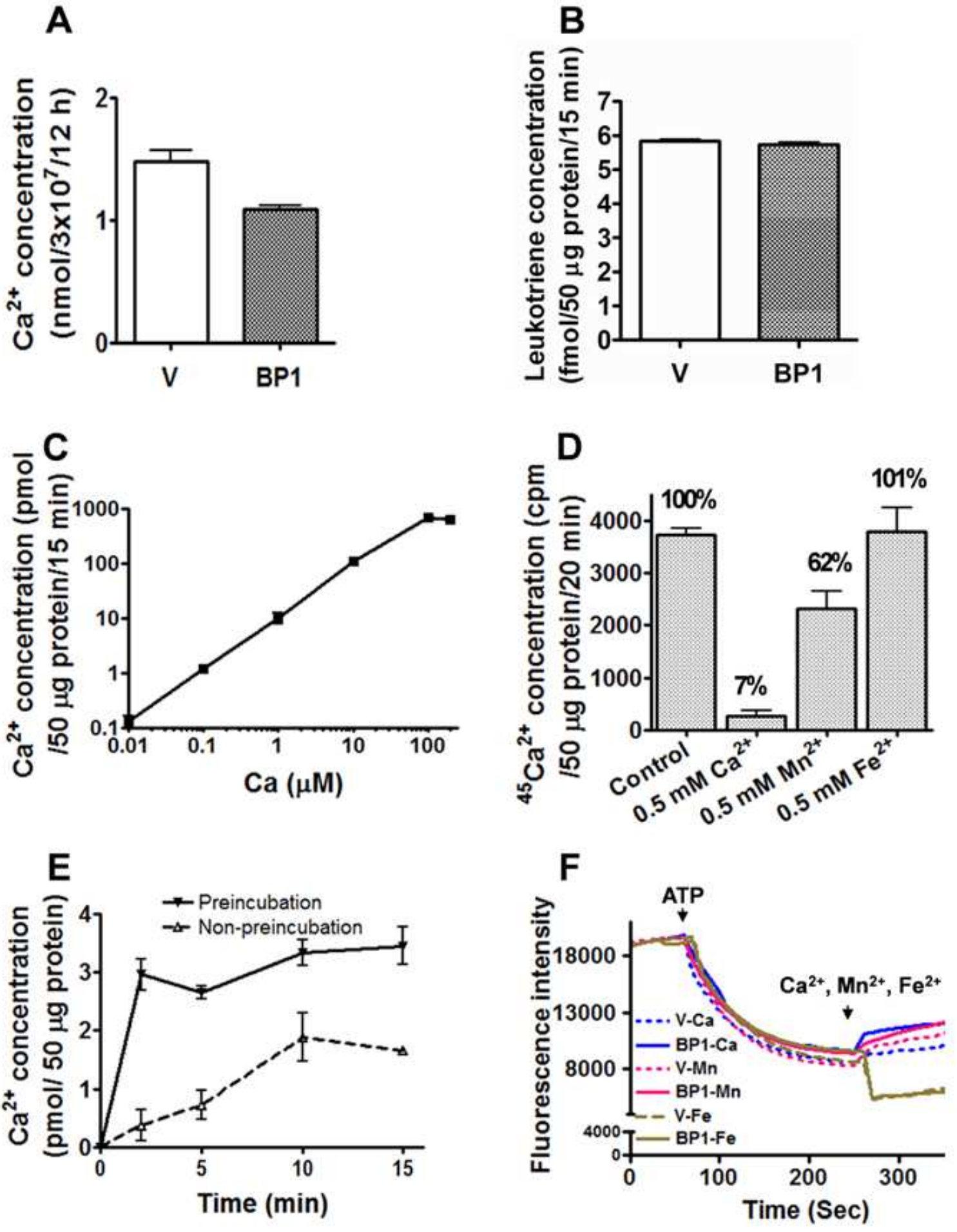
A
Ca2+ concentration (nmol/3x10^7/12 h)
2
1
0
V
BP1
B
Leukotriene concentration (fmol/50 μg protein/15 min)
7
6
5
4
3
2
1
0
V
BP1
C
Ca2+ concentration (pmol /50 μg protein/15 min)
1000
100
10
1
0.1
0.01
0.1
1
10
100
Ca (μM)
D
45Ca2+ concentration (cpm /50 μg protein/20 min)
4000
3000
2000
1000
0
100%
7%
62%
101%
Control
0.5 mM Ca2+
0.5 mM Mn2+
0.5 mM Fe2+
E
Ca2+ concentration (pmol/ 50 μg protein)
Preincubation
Non-preincubation
4
3
2
1
0
0
5
10
15
Time (min)
F
Fluorescence intensity
ATP
Ca2+, Mn2+, Fe2+
18000
13000
8000
4000
0
V-Ca
BP1-Ca
V-Mn
BP1-Mn
V-Fe
BP1-Fe
0
100
200
300
Time (Sec)

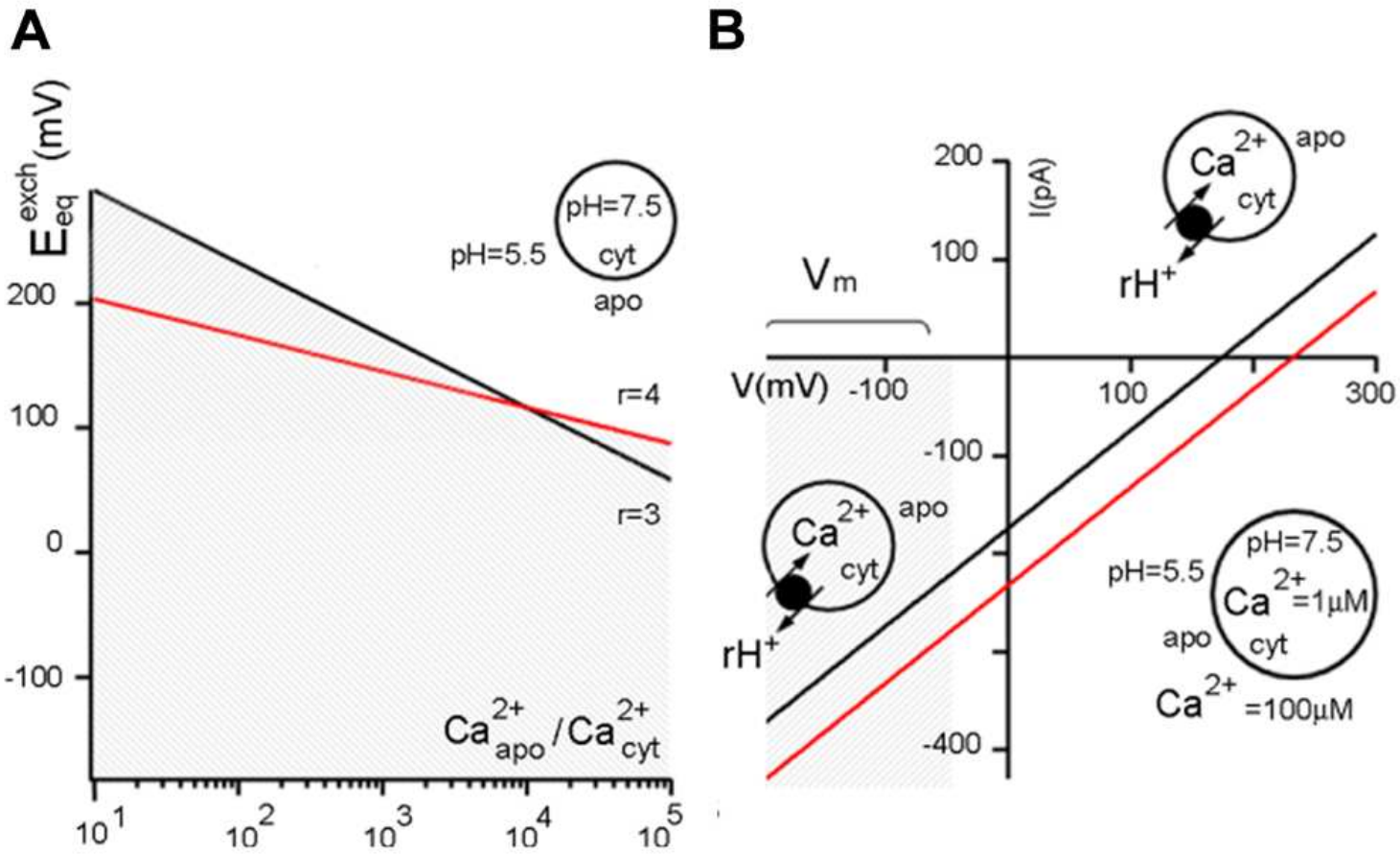
A
B
E_{eq}^{exch}(mV)
200
100
0
-100
r=4
r=3
pH=7.5
cyt
pH=5.5
apo
$Ca^{2+}_{apo}/Ca^{2+}_{cyt}$
10^1
10^2
10^3
10^4
10^5
I(pA)
200
100
-100
-400
V_m
V(mV) -100
100
300
Ca^{2+}
apo
cyt
rH^+
pH=7.5
pH=5.5
Ca^{2+}=1µM
apo
cyt
Ca^{2+} =100µM